1	HIGH-PRECISION AI-Mg ISOTOPIC SYSTEMATICS IN USNM 3898 – THE
2	BENCHMARK "ALL" FOR INITIAL 87Sr/86Sr IN THE EARLIEST SOLAR SYSTEM.
3	
4	
5	
6	
7	G. J. MacPherson <sup>1</sup> , C. Defouilloy <sup>2</sup> and N. T. Kita <sup>2</sup>
8	
9	
10	
11	
12	
13	<sup>1</sup> Dept. of Mineral Sciences, Museum of Natural History, Smithsonian Institution, Washington,
14	DC 20560, USA
15	
16	2W:-CDMC D
17	<sup>2</sup> WiscSIMS, Dept. of Geoscience, Univ. of Wisconsin-Madison, Madison, WI 53706, USA.
18	
19	
20	
21 22	Submitted to: Earth and Planetary Science Letters, Sept. 18, 2017
23	Submitted to. Earth and I tanetary Science Letters, Sept. 16, 2017
23	
25	
26	
20	

# 27281. Abstract

The Allende CAI *USNM 3898* is the basis for "ALL", the lowest measured initial  $^{87}$ Sr/ $^{86}$ Sr value in any solar system material including other CAIs (Gray *et al.* 1973). If the value ALL is correct (debated), then *USNM 3898* must be as much as 2 million years older than other CAIs (Podosek *et al.* 1991). This would require in turn that it have a much higher initial  $^{26}$ Al/ $^{27}$ Al value than other CAIs, on the order of  $4 \times 10^{-4}$ . Podosek *et al.* (1991) showed that this is not the case, with initial  $^{26}$ Al/ $^{27}$ Al =  $(4.5 \pm 0.7) \times 10^{-5}$ , but their Mg-isotopic data had large error bars and there was clear isotopic disturbance in the data having the highest  $^{27}$ Al/ $^{24}$ Mg. Without the latter data, the slope of their isochron is higher  $(5.10 \pm 1.19) \times 10^{-5}$ ) and within (large) error of being supracanonical. We used high-precision SIMS to re-determine the initial  $^{26}$ Al/ $^{27}$ Al in this CAI and obtained a value of  $(5.013\pm0.099) \times 10^{-5}$ , with an intercept  $\delta^{26}$ Mg\* = -0.008±0.048 and MSWD = 1.3. This value is indistinguishable from that measured in many other CAIs and conclusively shows that *USNM 3898* is not uniquely ancient. We also confirmed evidence of later isotopic disturbance, similar to what Podosek *et al.* found, indicating a re-melting and evaporation event some 200,000 years after initial CAI solidification.

# 2. Introduction

During the 1960s and 1970s, several reference values for initial <sup>87</sup>Sr/<sup>86</sup>Sr during the early Solar System were defined in the laboratories of Prof. G. J. Wasserburg at Caltech, based on analyses of meteorites. These included "BABI" (Basaltic Achondrite Best Initial; Papanastassiou and Wasserburg, 1969), ADOR (Angra dos Reis; Papanastassiou, 1970; Wasserburg *et al.* 1977) and ALL (Allende; Gray *et al.* 1973). Of these the lowest value is that of ALL, and this was taken to be the Solar System initial value when solids first began forming in the solar nebula (but see recent studies challenging this assumption, e.g. Moynier *et al.* 2012; Hans *et al.* 2013).

The value ALL is from an analysis of a single calcium-aluminum-rich inclusion (CAI), specifically a compact Type A CAI from the Allende CV3 chondrite labelled *USNM 3898* but referred to by Gray *et al.* (1973) as their sample D7 (the equivalence is stated explicitly by Niederer and Papanastassiou, 1984; henceforth, we will refer to it simply as *USNM 3898*). The Rb-Sr isotopic systematics of *USNM 3898* were later re-examined by Papanastassiou and Wasserburg (1978), Podosek *et al.* (1991), and Papanastassiou and Chen (2017). Papanastassiou and

Wasserburg (1978) re-analyzed some remaining material from USNM 3898 and determined a 57 somewhat higher value for its initial <sup>87</sup>Sr/<sup>86</sup>Sr than that determined by Gray et al. (1973). In addi-58 tion to Rb-Sr, Podosek et al. (1991) also studied Mg isotopes via secondary ionization mass 59 spectrometry (SIMS). The Podosek et al. results were curious for two reasons. First, their value 60 for initial <sup>87</sup>Sr/<sup>86</sup>Sr was not the same as that obtained by Gray et al. (1973) on a different frag-61 ment of the same CAI, but instead somewhat higher. Their measured <sup>87</sup>Rb/<sup>86</sup>Sr also was some-62 what higher than that determined by Gray et al (1973), possibly due to a higher proportion of ma-63 terial from nearer the rim of the CAI where most of the secondary minerals reside. Second, the 64 Al-Mg isotope data gave a somewhat-disturbed isochron for which all data vielded initial 65  $^{26}\text{Al}/^{27}\text{Al} = (4.5 \pm 0.7) \times 10^{-5}$  (for reasons discussed later, even within its own error limits this val-66 ue is not so well determined as it seems). Although just within error of the Solar System initial 67 value of  $^{26}\text{Al}/^{27}\text{Al} = (5.23 \pm 0.13) \times 10^{-5}$  (Jacobsen et al. 2008), if taken at face value the value ob-68 tained by Podosek et al. (1991) for USNM 3898 is somewhat lower than that many CV3 CAIs. 69 Yet if USNM 3898 is the oldest object in the Solar System as implied by its initial 87Sr/86Sr val-70 ue, it should have the highest initial <sup>26</sup>Al/<sup>27</sup>Al (assuming nebular homogeneity of strontium iso-71 topes). In fact, as Podosek et al. (1991) noted, the low initial 87Sr/86Sr value ALL relative to oth-72 er measured CAIs requires USNM 3898 to be on the order of 1 million years older than other 73 measured CAIs. This in turn would imply a supracanonical initial <sup>26</sup>Al/<sup>27</sup>Al value for this CAI, 74 roughly  $1 \times 10^{-4}$ . In part because this is not what they observed, Podosek et al. (1991) concluded 75 that the correct initial <sup>87</sup>Sr/<sup>86</sup>Sr value for ALL is somewhat higher than calculated by Gray *et al.* 76 (1973) and nearer to the upper limits of its error bars, which would make it contemporaneous 77 with other CAIs. More recent work (discussed below) on other CAIs has demonstrated the pres-78 ence of strontium isotope anomalies in CAIs and examined the possible consequences for chron-79 ological significance of initial <sup>87</sup>Sr/<sup>86</sup>Sr values in CAIs in general (Moynier et al. (2012) and 80 Hans et al. (2013); Charlier et al. 2017, Paton et al. 2013) 81

Lost in much of this is *USNM 3898* itself. Since the Podosek *et al.* study, new insights have prompted us to reconsider both the formation of this particular CAI and its Al-Mg isotopic systematics. Specifically, the presence of a very aluminum-rich outer mantle on *USNM 3898* is important for two reasons. First, new theoretical ideas and experimental results relating to the role of melt evaporation in the evolution of CAIs in general (Grossman *et al.* 2000; Richter *et al.* 2002; Richter *et al.* 2007) are a hint that this CAI may have experienced a late episode of that

82

83

84

85

86

phenomenon. Second, the Mg-isotopic data reported by Podosek et al. (1991) are tightly isochronous except for two data points taken from the aluminous outer mantle. One point plots significantly below the isochron calculated by those authors, and a second is below but within error of the isochron. If these points are excluded from the slope calculation, the inferred initial <sup>26</sup>Al/<sup>27</sup>Al value is  $(5.10\pm1.19)\times10^{-5}$ , possibly supracanonical albeit not within error of the putative value implied by the Sr isotope ratio ALL. Thus we decided to re-determine more definitively the initial <sup>26</sup>Al/<sup>27</sup>Al of this CAI at the time of its formation, with particular attention paid to distinguishing the outer mantle of the CAI from its interior. Specifically, is the initial <sup>26</sup>Al/<sup>27</sup>Al value of the CAI interior supracanonical and therefore consistent with the antiquity of D7 / USNM 3898 relative to other CAIs that is implied by the value ALL, or not? Our high-precision and detailed study takes advantage of the superior capabilities of the latest generation SIMS instruments such as the ims-1280. The new data show that the interior phases of USNM 3898 (i.e. excluding the outer mantle) define an isochron that unequivocally is not supracanonical, and thus is inconsistent with the putative <sup>87</sup>Sr/<sup>86</sup>Sr difference between ALL and other CAIs. Data from the outer mantle consistently plot below this isochron, hinting at a late stage of melt evaporation that occurred ~200,000 years after primary CAI solidification

# 3. Sample Description

USNM 3898 is a Compact Type A inclusion composed mostly of melilite, with accessory spinel, pyroxene, and the rare mineral rhönite. It was analyzed for major and trace elements by Mason and Martin (1977), and briefly described by Mason and Taylor (1980) and Teshima and Wasserburg (1985). Fagan et al. (2007) reported Al-Mg isotopic data for secondary phases. A much more complete description along with a BSE image is given in Podosek et al. (1991). Figure 1 shows paired BSE and Ca-Al-Mg elemental maps of this ~0.7 cm elliptical CAI, and Figures 2 and 3 show more detailed BSE images. That complete sample description need not be repeated here, but several critical points require emphasis. First, the interior of the CAI is largely free of secondary alteration. This fact accounts for the very low Rb/Sr value measured by Gray et al. (1973), and which is why this CAI was used to constrain the initial Solar System value for <sup>87</sup>Sr/<sup>86</sup>Sr. Virtually all secondary alteration is confined to within a few hundred microns of the CAI outermost margin (Fig. 2). Second, and as pointed out by Podosek et al. (1991), several petrologic features of USNM 3898 are inconsistent with a simple melt crystallization model implied by its deceptively elliptical shape. These include monotonically-reversed compositional zoning

of individual melilite crystals (see Fig. 5 of Podosek et al, 1991), an outer surface that is highly irregular at a fine scale and might best be described as "frittered" (Fig. 2), and melilite just below the Wark-Lovering rim sequence (Fig. 3) that is significantly more aluminous ( $Åk_{0-10}$ ) than any melilite in the inclusion interior ( $Åk_{10-35}$ ). This latter feature hints at (albeit does not prove) melt evaporation from the surface of the CAI while it was molten.

#### 4. Analytical Methods

Candidate grains for SIMS study were selected and carefully documented prior to isotopic analysis using the FEI NOVA NanoSEM 600 scanning electron microscope (SEM) at the Smithsonian Institution.

Aluminum-magnesium isotopic analyses were performed using the WiscSIMS Cameca ims 1280 at the University of Wisconsin-Madison, using techniques similar to those described in Kita *et al.* (2012) and MacPherson *et al.* (2017). All minerals in the CAIs (melilite, spinel, rhönite, and pyroxene) were analyzed by using multicollection Faraday cups (FC). Data were corrected for intrinsic mass-dependent fractionation using an exponential law:

$$\delta^{26} M g^* = \delta^{26} M g - \left[ \left( 1 + \frac{\delta^{25} M g}{1000} \right)^{\frac{1}{\beta}} - 1 \right] \times 1000$$

where  $\beta = 0.5128$ , the value recommended by Davis et al. (2015; see for details). Additional details of the procedures for data reduction at the University of Wisconsin are given in Ushikubo et al. (2017).

After SIMS analysis, each ion probe pit was imaged using an SEM to check for any overlap onto other mineral phases or cracks, which, if found, led to their rejection.

One important concern was minimizing spot size for maximum spatial resolution. The primary  $O^-$  beam was tuned to a uniform oval shape (0.8 aspect ratio; Köhler illumination) using mass apertures and beam apertures in the primary column. The primary beam diameter and intensity were optimized for each phase and grain size by applying different combinations of aperture sizes, which increased somewhat during the session due to sputtering by the primary beam. The spot sizes (long dimension) and conditions were as follows:  $10 \mu m$  (5-6 nA) for spinel, pyroxene, and rhönite analyses, and 15– $20 \mu m$  (20 nA) for melilite analyses.

Each analysis duration was  $\sim 8$  minutes. Matrix matched Mg-isotope standards of spinel, fassaite glass and melilite glass (with known  $\delta^{25}$ Mg values except for spinel; Kita *et al.* 2012; Ushikubo *et al.* 2017) were analyzed multiple times during each session in order to bracket unknown analyses. The analyses of rhönite was performed by using fassaite standard. The external reproducibility (2SD) of  $\delta^{25}$ Mg analyses was typically 0.1–0.2% for these standards except for  $\sim 0.5\%$  for Al-rich melilite. The external reproducibility of  $\delta^{26}$ Mg\* in the standards was 0.07–0.15% for spinel, Mg-rich melilite and pyroxene analyses, while that of melilite analyses was typically 0.2–0.3% for Mg-rich melilite and degraded to  $\sim 1.0\%$  for Al-rich melilite. The internal errors of each standard analysis are generally similar to or slightly worse than those of external reproducibility given above, so that final uncertainties of unknown analyses are propagated from both internal errors of individual analyses and the uncertainty of mean matching standards that bracket the unknown analyses.

#### 5. Results

### 5.1 Initial $^{26}Al/^{27}Al$

All isotopic data are given in Table 1. Figures 4a-d are isochron diagrams that show our isotopic data for spinel, pyroxene, rhönite, and melilite at different axis scales to resolve low  $^{27}\text{Al}/^{24}\text{Mg}$  phases from high  $^{27}\text{Al}/^{24}\text{Mg}$  phases. Figure 4a shows all data for interior phases (i.e. excluding only the outermost aluminous melilite). These data, again excluding the outermost melilite, collectively define a very coherent isochron having a slope that corresponds to initial  $^{26}\text{Al}/^{27}\text{Al} = (5.013\pm0.099)\times10^{-5}$ , with MSWD = 1.3 and an intercept  $\delta^{26}\text{Mg*} = -0.008\pm0.048$ . Figures 4b and 4c show the same data but at larger scale to show in detail the data for phases with  $^{27}\text{Al}/^{24}\text{Mg} < 20$ . Even the phases with the lowest  $^{27}\text{Al}/^{24}\text{Mg}$  (rhönite, spinel, and pyroxene) data adhere closely to the same isochron defined in Fig. 4a. Figure 4d includes the data for the most aluminous melilite ( $^{27}\text{Al}/^{24}\text{Mg} \sim 66$ ) that occurs just beneath the Wark-Lovering rim. These data points fall below the line defined by all other data; one is just marginally within error of the line but the second data point is clearly resolved from it.

Also shown in Fig. 4d are the melilite data from Podosek *et al.* (1991). The latter data are consistent with our own, but with much larger error bars. The most interesting aspect of Fig. 4d is the fact that the two most aluminous melilite points of the Podosek *et al.* data plot below (one within error, the other not) the line defined by our data for the interior phases, in the same way

that our own most aluminous melilites do. And again, those two most aluminous melilites from the Podosek *et al.* data are from the outermost region of the CAI. Fitting a correlation line to their data that excludes these two aluminous melilite points yields initial  $^{26}$ Al/ $^{27}$ Al =  $(5.104 \pm 1.186) \times 10^{-5}$ . Given the large error on the slope, this ratio is within error of being supracanonical. Our more precise data rule this possibility out.

In our treatment of both our own data and that of Podosek et al. (1991), we are not arbitrarily choosing what data to include or not include in the regressions. For both, the only data to lie significantly off the regression line are the aluminous melilite points from the outer portion of the CAI. The correlation of isotopic signature with the anomalously aluminum-rich nature of this outer mantle can hardly be a coincidence.

## 5.2 Mg Intrinsic Mass Fractionation

Figure 5 shows intrinsic mass-dependent fractionation of magnesium (i.e. corrected for instrumental effects), calculated as  $\delta^{25}$ Mg. Figure 5a gives the data for all phases, showing that all interior phases, including magnesium-rich melilite, are consistently enriched in heavy magnesium isotopes at  $\delta^{25}$ Mg ~5–8. For comparison, Niederer and Papanastassiou (1984) obtained a bulk value for *USNM 3898* of 9 (see their Table 4). However, the very aluminous melilite near the inclusion margin shows about ½ the degree of heavy isotope enrichment relative to the center. Figure 5b shows only the melilite data, plotted as a function of melilite composition. The correlation is approximately linear. Taken in the context of melt evaporation from the CAI margin while it was molten, the patterns in Figs. 5a, b are precisely the opposite of that expected. As noted in the Discussion, however, this in fact is a relatively common pattern.

#### 6. Discussion

Podosek *et al.* (1991) concluded from their SIMS data that initial <sup>26</sup>Al/<sup>27</sup>Al in *USNM 3898* is not supracanonical. However, if their data for the most aluminous melilite is excluded from the slope calculation, then their inferred initial <sup>26</sup>Al/<sup>27</sup>Al in fact is within (large) error of being significantly supracanonical – to be expected if the correct value for initial <sup>87</sup>Sr/<sup>86</sup>Sr is in fact ALL and not that determined in their own study. Our new and far more precise SIMS data definitively rule out a supracanonical slope. Indeed *USNM 3898* is well within error of both the "old" canonical

value for initial  $^{26}$ Al/ $^{27}$ Al (5 × 10<sup>-5</sup>) and the new more precise estimate of (5.23 ± 0.13) × 10<sup>-5</sup> (Jacobsen *et al.* 2008). Thus the problem pointed out by Podosek *et al.* (1991) – inconsistency between the initial  $^{87}$ Sr/ $^{86}$ Sr of *USNM 3898* (ALL) and its initial  $^{26}$ Al/ $^{27}$ Al – is reinforced by our work. If *USNM 3898* is the oldest object formed in the Solar System, as Gray *et al.*'s determination of its initial  $^{87}$ Sr/ $^{86}$ Sr value (ALL) would seem to indicate, then it also should have the highest initial  $^{26}$ Al/ $^{27}$ Al value (unless it formed prior to injection of  $^{26}$ Al, in which case the initial value should be close to zero). Neither is the case. Rather, its initial  $^{26}$ Al/ $^{27}$ Al value is typical of the majority of CV3 CAIs.

Although outside of the scope of the present paper, a few words about the strontium isotopic composition of USNM 3898 and the significance of ALL are merited here in the interest of context. Our new data confirm the conclusion of Podosek et al. (1991) that, solely from a magnesium isotopic point of view, USNM 3898 is not older than any other CAIs. Based on their own data, Podosek et al. (1991) concluded that the value "ALL" is not the correct value for D7=USNM 3898. They argued that a more accurate value for CAI (hence Solar System) initial <sup>87</sup>Sr/<sup>86</sup>Sr is 0.69881, which was derived from another Allende CAI (USNM 3529-Z) measured in their same study. However, the entire debate over ALL and solar system initial <sup>87</sup>Sr/<sup>86</sup>Sr would be moot if a recent suggestion by Moynier et al. (2012) and Hans et al. (2013) is correct. They showed that many CAIs possess an apparent excess in <sup>84</sup>Sr, a non-radiogenic isotope. This has two possible consequences. First, the anomaly in <sup>84</sup>Sr casts doubt on the nebular homogeneity assumption with respect to age considerations. Second, the observed effects in <sup>84</sup>Sr could equally be effects of the same sign in <sup>88</sup>Sr, which is one of the isotopes used for normalization in Sr-isotopic determinations. This would require significant corrections to all previous values of <sup>87</sup>Sr/<sup>86</sup>Sr in CAIs. This issue remains open, but Papanastassiou and Chen (2016) give quantitative arguments why the apparent anomalies in <sup>84</sup>Sr are unlikely to be due to anomalies in <sup>88</sup>Sr.

Turning now to the internal isotopic systematics of *USNM 3898*, the outermost melilite is not isochronous with the interior phases (in either our data set or that of Podosek et *al.* 1991). Using just our data set, including the aluminous melilite with all of the other data yields a lower slope that corresponds to initial  $^{26}$ Al/ $^{27}$ Al =  $(4.567\pm0.114)\times10^{-5}$ . Alternatively, Fig. 5 shows that fitting those outer points to either the bulk  $^{27}$ Al/ $^{24}$ Mg of *USNM 3898* or to the  $^{27}$ Al/ $^{24}$ Mg of the most aluminous *concordant* melilite (Åk ~8) yields yet lower slopes that correspond to  $^{26}$ Al/ $^{27}$ Al  $\sim 4.5 \times 10^{-5}$  or  $\sim 4.2 \times 10^{-5}$  respectively. This outermost melilite obviously records a later event

than the interior of *USNM 3898*. There is very little secondary alteration in *USNM 3898* at all, and post-analysis imaging of the SIMS spots by SEM showed that that those outer melilite spots are uncontaminated. Thus we conclude that the isotopic signatures of this outer melilite record a later heating event that melted the outer margins of the CAI and, by implication, evaporated substantial magnesium from the melt to form the aluminous mantle melilite. This later event occurred on the order of 200,000 years after original solidification of the CAI interior.

The problem with this model is evident in Figure 6. Melt evaporation at the surface of a molten CAI will enrich the remaining melt in  $^{25}$ Mg relative to  $^{24}$ Mg, yet precisely the opposite is observed in USNM 3898. It is the magnesium-rich cores of the interior melilite crystals that are most enriched in  $^{25}$ Mg and all other melilite (including the outermost aluminous melilite) shows a lower degree of mass-dependent isotopic fractionation. This same pattern has been observed in other CAIs that – based on more definitive petrologic evidence than that in USNM 3898 – also are thought to have undergone surface melt evaporation (Bullock *et al.* 2013). The main difference between the two studies is that, in three of the Type B CAIs studied by Bullock and colleagues,  $\delta^{25}$ Mg did not vary so smoothly as a function of melilite composition (the fourth showed no clear covariation at all). Rather,  $\delta^{25}$ Mg decreased sharply at compositions more aluminous than  $\Delta^{25}$ Mg. That clearly is not the case here but, nevertheless, in both studies the most aluminous melilites generally exhibited the least degree of enrichment in  $\Delta^{25}$ Mg. So far in fact, of the CAIs studied anywhere, the sole example of unambiguous heavy Mg isotope enrichment in the outer margin of a CAI is that reported by Shahar and Young (2007).

Like Bullock *et al.* (2013), we have no easy explanation for this contradiction between the isotopic and petrologic evidence. However, regardless of whether *USNM 3898* actually did experience localized melt evaporation, the inclusion margin must have experienced later magnesium isotopic exchange with an external and isotopically-lighter reservoir. If the margin was originally enriched in <sup>25</sup>Mg relative to the CAI interior, then the exchange reversed that pattern.

#### 7. Conclusions

Our high-precision Mg isotopic data show that *USNM 3898*, the CAI having the lowest initial  $^{87}$ Sr/ $^{86}$ Sr of any measured Solar System material (including other CAIs), has an initial  $^{26}$ Al/ $^{27}$ Al ratio (5.013±0.099) × 10<sup>-5</sup> that is indistinguishable from the currently accepted "canonical" initial Solar System ration of (5.23 ± 0.13) × 10<sup>-5</sup> (Jacobsen *et al.* 2008). This argues against *USNM* 

3898 being significantly older than any other CAI, as noted previously by Podosek *et al.* (1991), and independently of any argument based on initial <sup>87</sup>Sr/<sup>86</sup>Sr ratios in this or any other CAI.

### 8. Acknowledgements

This research was supported by National Aeronautics and Space Administration (NASA) grant NNX15AH68G (GJM, PI). WiscSIMS is partly supported by National Science Foundation grants EAR03-19230 and EAR13-55590. Drs. Dimitri Papanastassiou, Bernard Bourdon, and an anonymous reviewer provided reviews that substantially improved the paper. Comments by the anonymous reviewer in particular and Associate Editor Frederick Moynier led us to re-focus the paper in a more significant direction.

- Brennecka G. A., Borg L. E., and Wadhwa M. (2013) Evidence for supernova injection into the solar nebula and the decoupling of r-process nucleosynthesis. *Proc. Nat. Acad. Sci.* **110**: 17241–17246.
- Bullock E. S., Knight K. B., Richter F. M., Kita N. T., Ushikubo T., Davis A. M., MacPherson G. J., Mendybaev R. A. (2013) Evaporation conditions inferred from Mg and Si isotopic fractionation in melilite from Type B1 and B2 CAIs. *Meteoritics and Planetary Science* 48, 1440–1458.
- Charlier B.L.A., Parkinson I.J., Burton K.W., Grady M.M., Wilson C.J.N., and Smith E.G.C.
   (2017) Stable strontium isotopic heterogeneity in the solar system from double-spike data.
   *Geochemical Perspectives Letters* 4: 35-40
- Davis A. M., Richter F. M., Mendybaev R. A., Janney P. E., Wadhwa M. and McKeegan K. D. (2015) Isotopic mass fractionation laws for magnesium and their effects on <sup>26</sup>Al–<sup>26</sup>Mg systematics in solar system materials. *Geochimica et Cosmochimica Acta* **158**, 245–261.
- Fagan T.J., Guan Y. and MacPherson G.J. (2007) Al-Mg isotopic evidence for episodic alteration of Ca-Al-rich inclusions from Allende. *Meteoritics and Planetary Science* **42**, 1221-1240.
- Gray C. M., Papanastassiou D. A. and Wasserburg G. J. (1973) The identification of early condensates from the solar nebula. *Icarus* 20:213–239.
- Grossman L, Ebel, D. S., Simon S. B., Davis A. M.; Richter, F. M. and Parsad, N. M. 2000. Major element chemical and isotopic compositions of refractory inclusions in C3 chondrites:
  The separate roles of condensation and evaporation. *Geochimica et Cosmochimica Acta* **64**, 2879-2894.
- Hans U., Kleine T., and Bourdon B. (2013) Rb–Sr chronology of volatile depletion in differentiated protoplanets: BABI, ADOR and ALL revisited. *Earth and Planetary Science Letters* 303 **374**: 204–214.
- Jacobsen B., Yin Q.-Z., Moynier F., Amelin Y., Krot A. N., Nagashima K., Hutcheon I. D. and Palme H. (2008) 26Al–26Mg and 207Pb–206Pb systematics of Allende CAIs: canonical solar initial 26Al/27Al ratio reinstated. *Earth and Planetary Science Letters* **272**, 353–364.
- Kita N. T., Ushikubo T., Knight K. B., Mendybaev R. A., Davis A. M., Richter F. M. and Fournelle J. H. (2012) Internal <sup>26</sup>Al-<sup>26</sup>Mg isotope systematics of a Type B CAI: remelting of refractory precursor solids. *Geochim. Cosmochim. Acta* **86**, 37–51.
- MacPherson G. J., Tenner T. J., Nakashima D., Kita N. T., Bullock E. S., Ivanova M. A., Krot A. N., Petaev M. I., and Jacobsen S. B. (2017) High precision Al-Mg systematics of forsterite-bearing Type B CAIs from CV3 chondrites. *Geochimica et Cosmochimca Acta*. **201**, 65–82.
- Mason B. and Martin P.M. (1977) Geochemical differences among components of the Allende meteorite. *In Mineral Sciences Investigations*, ed. B. Mason, *Smithson. Contrib. Earth Sci.* **19,** 84-95.
- Mason B. and Taylor S.R. (1982) Inclusions in the Allende meteorite. *Smithson. Contrib. Earth Sci.* **25,** 30 pp.

- Moore L. J., Murphy T. J., Barnes I. L., and Paulsen P. J. (1982) Absolute isotopic abundance ratios and atomic weight of a reference sample of strontium. *J. Res. NBS* **87** (8 pp.).
- Moynier F., Day J. M. D., Okui W., Yokoyama T., Bouvier A., Walker R. J., and Podosek F. A.
- (2012) Planetary-scale strontium isotopic heterogeneity and the age of volatile depletion of
- early solar system materials. *Ap. J.* **758**: 45-51.
- Niederer F.R. and Papanastassiou D.A. (1984) Ca isotopes in refractory inclusions. *Geochimica et Cosmochimica Acta* **48**: 1279-1294.
- Papanastassiou D. A. and Wasserburg G. J. (1978) Strontium isotopic anomalies in the Allende meteorite. *Geophysical Research Letters* 5: 595-598.
- Papanastassiou D. A. and Chen J. H. (2016). Initial <sup>87</sup>Sr/<sup>86</sup>Sr chronology in the solar system. *47th Lunar and Planetary Science Conference* (abstract #2650)
- Paton C., Schiller M., and Bizzarro M. (2013) Identification of an <sup>84</sup>Sr-depleted carrier in primitive meteorites and implications for thermal processing in the solar protoplanetary disk. The *Astrophysical Journal Letters* **763**: L40 (6pp)
- Podosek F.A., Zinner E.K., MacPherson G.J., Lundberg L., Brannon J.C. and Fahey A.F. (1991)
  Correlated study of initial <sup>87</sup>Sr/<sup>86</sup>Sr and Al-Mg isotopic systematics and petrologic properties
- in a suite of refractory inclusions from the Allende meteorite. *Geochim. Cosmochim. Acta*, v.
- **55**, 1083-1110.

- Richter F. M., Davis A. M., Ebel D. S. and Hashimoto A. 2002. Elemental and isotopic frac-
- tionation of Type B calcium-, aluminum-rich inclusions: experiments, theoretical considera-
- tions, and constraints on their thermal evolution. *Geochimica et Cosmochimica Acta* 66, 521-540.
- Richter F. M., Janney P. E., Mendybaev R. A., Davis A. M., and Wadhwa M. 2007b. Elemental and isotopic fractionation of Type B CAI-like liquids by evaporation. *Geochimica et Cosmochimica Acta* 71, 5544–5564.
- Shahar A. and Young E. D. 2007. Astrophysics of CAI formation as revealed by silicon isotope LA-MC-ICPMS of an igneous CAI. *Earth and Planetary Science Letters* **257**:497–510.
- Teshima J. and Wasserburg G.J. (1985) Textures, metamorphism and origin of type A CAI's. *Lunar Planet. Sci. XVI* 855-856.
- Ushikubo T., Kimura M., Kita N. T. and Valley J. W. (2012) Primordial oxygen isotope reservoirs of the solar nebula recorded in chondrules in Acfer 094 carbonaceous chondrite. *Geochim. Cosmochim. Acta* **90**, 242–264.
- Ushikubo T., Tenner T. J., Hiyagon H., and Kita N. T. (2017) A long duration of the <sup>16</sup>O-rich reservoir in the solar nebula, as recorded in fine-grained refractory inclusions from the least metamorphosed carbonaceous chondrites. *Geochimica et Cosmochimica Acta* **201**: 103–122

	<sup>27</sup> Al/ <sup>24</sup> Mg	2σ	Åk (mel)*	$\delta^{26}$ Mg*	2σ	$\delta^{25}$ Mg	2σ
Area 1 Mel 1	13.498	0.135	16	4.829	0.187	3.042	0.479
Area 1 Mel 2	10.845	0.110	19	4.074	0.163	3.366	0.479
Area 1 Mel 3	8.667	0.087	23	3.090	0.167	5.829	0.479
Area 1 Mel #4	7.547	0.075	25	2.624	0.149	5.314	0.479
Area 1 Mel #5	28.285	0.290	8	9.645	0.351	2.403	0.479
Area 2 Mel #6	66.341	1.670	4	21.035	1.021	1.305	0.479
Area 2 Mel #7	8.249	0.083	23	3.036	0.173	4.946	0.479
Area 2 Mel #8	65.927	0.691	4	22.201	0.982	2.067	0.479
Area 3 Mel #9	15.419	0.155	14	5.522	0.198	2.272	0.479
Area 3 Mel #10	25.441	0.265	9	9.393	0.408	2.689	0.479
Area 3 Mel #11	16.418	0.164	13	5.965	0.247	3.654	0.479
Area 4 Mel #12	7.638	0.076	25	2.736	0.176	6.224	0.479
Area 4 Mel #13	7.722	0.077	25	2.900	0.169	6.060	0.479
Area 7 Pyx #1	3.378	0.034		1.258	0.197	5.814	0.433
Area 6 Pyx #2	3.636	0.036		1.136	0.197	6.073	0.433
Area 6 Pyx #3	3.861	0.039		1.503	0.207	5.860	0.433
Area 5 Pyx #4	3.969	0.040		1.383	0.197	6.259	0.433
Area 5 Pyx #5	3.728	0.037		1.230	0.197	6.446	0.433
Area 5 Rhönite #1	1.994	0.020		0.737	0.197	5.463	0.433
Area 4 Sp #1	2.531	0.025		0.888	0.088	7.298	0.049
Area 4 Sp #2	2.519	0.025		0.879	0.088	7.667	0.049
Area 4 Sp #3	2.511	0.025		0.913	0.088	7.666	0.049
Area 4 Sp #4	2.517	0.025		0.883	0.088	7.568	0.049

<sup>\*</sup> Melilite composition expressed as mole % åkermanite (Ca<sub>2</sub>MgSi<sub>2</sub>O<sub>7</sub>)

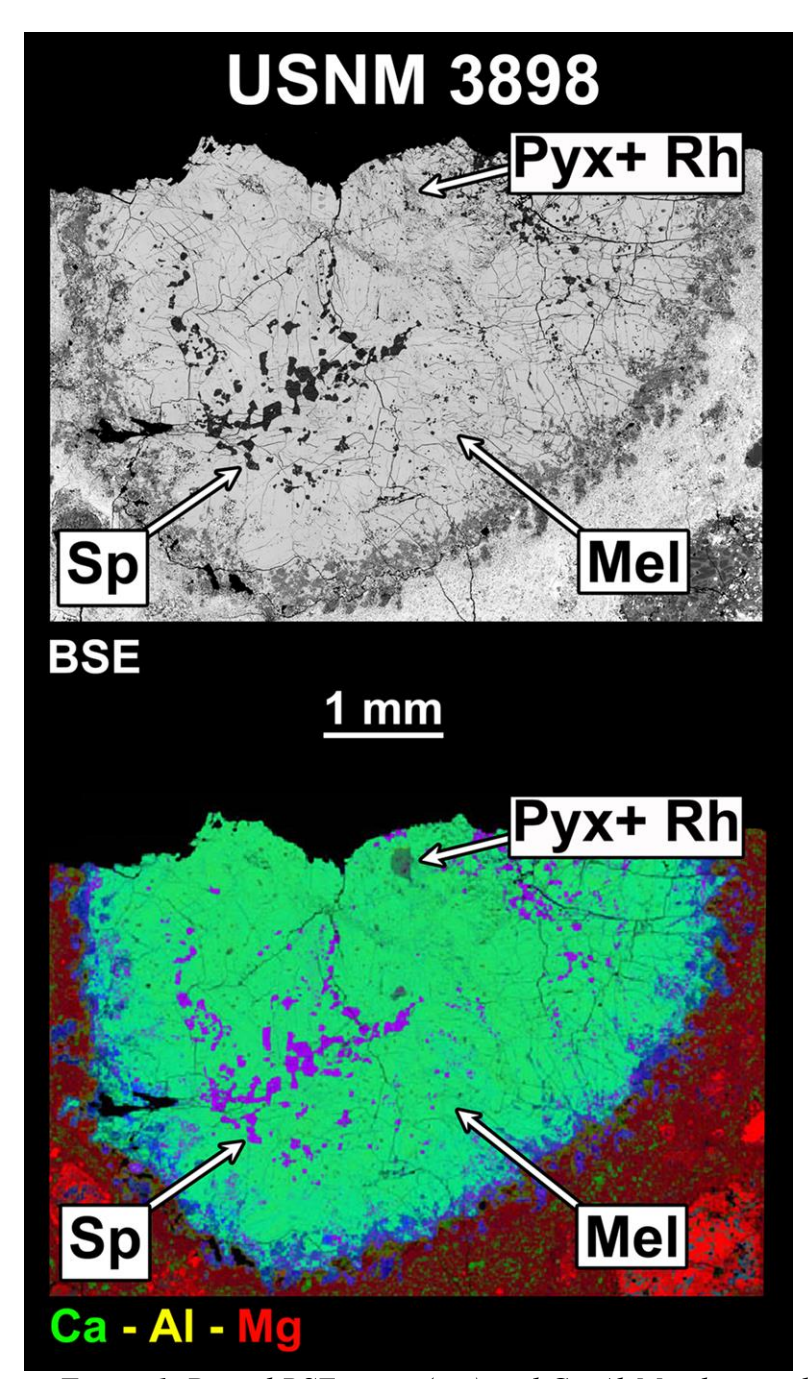


Figure 1. Paired BSE mage (top) and Ca-Al-Mg element distribution map (bottom) of USNM 3898. In the lower image, melilite (Mel) is greenish aqua blue, spinel (Sp) is magenta, pyroxene and rhönite (Pyx + Rh) are olive, and the dark blue material around the margin is a mixture of fine-grained secondary anorthite, nepheline, and sodalite.

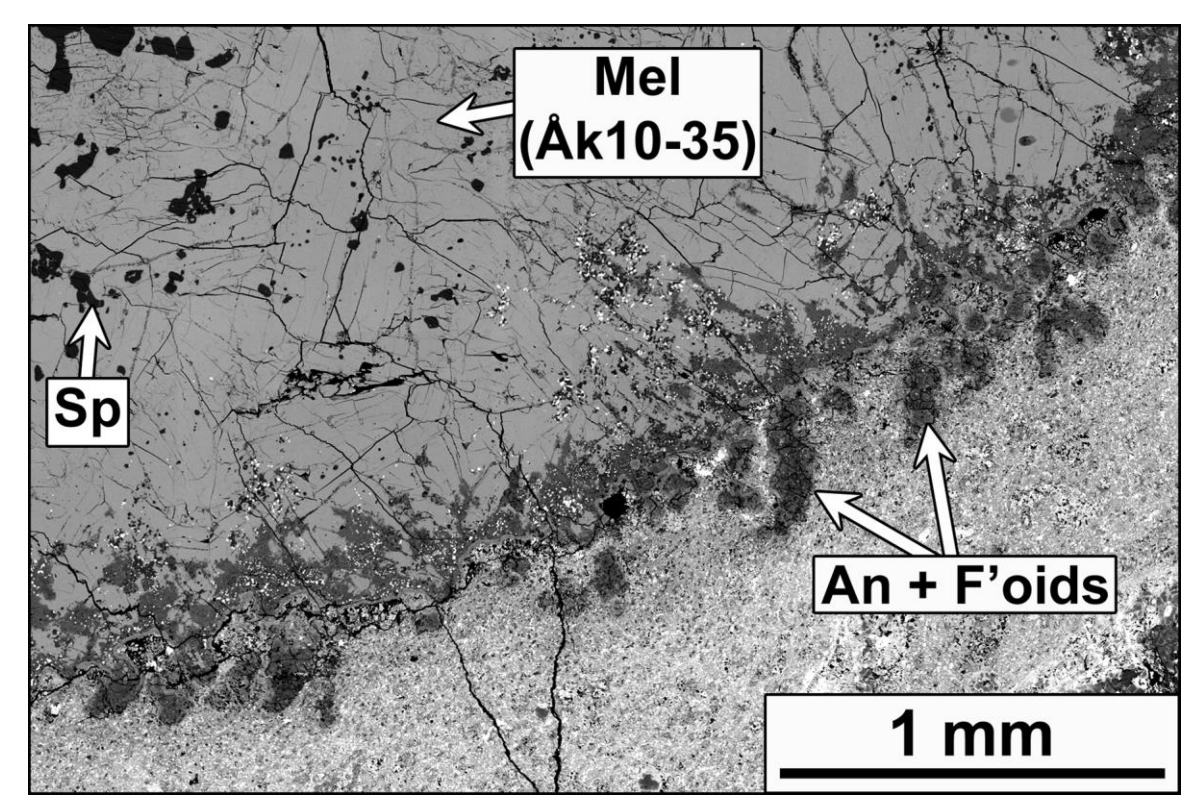


Figure 2. BSE image or a portion of the outer margin of USNM 3898, showing the "frittered" nature. Most of the material in the "fingers" consists of secondary anorthite (An) and the feld-spathoids (F'oids) nepheline and sodalite, along with minor spinel (Sp).

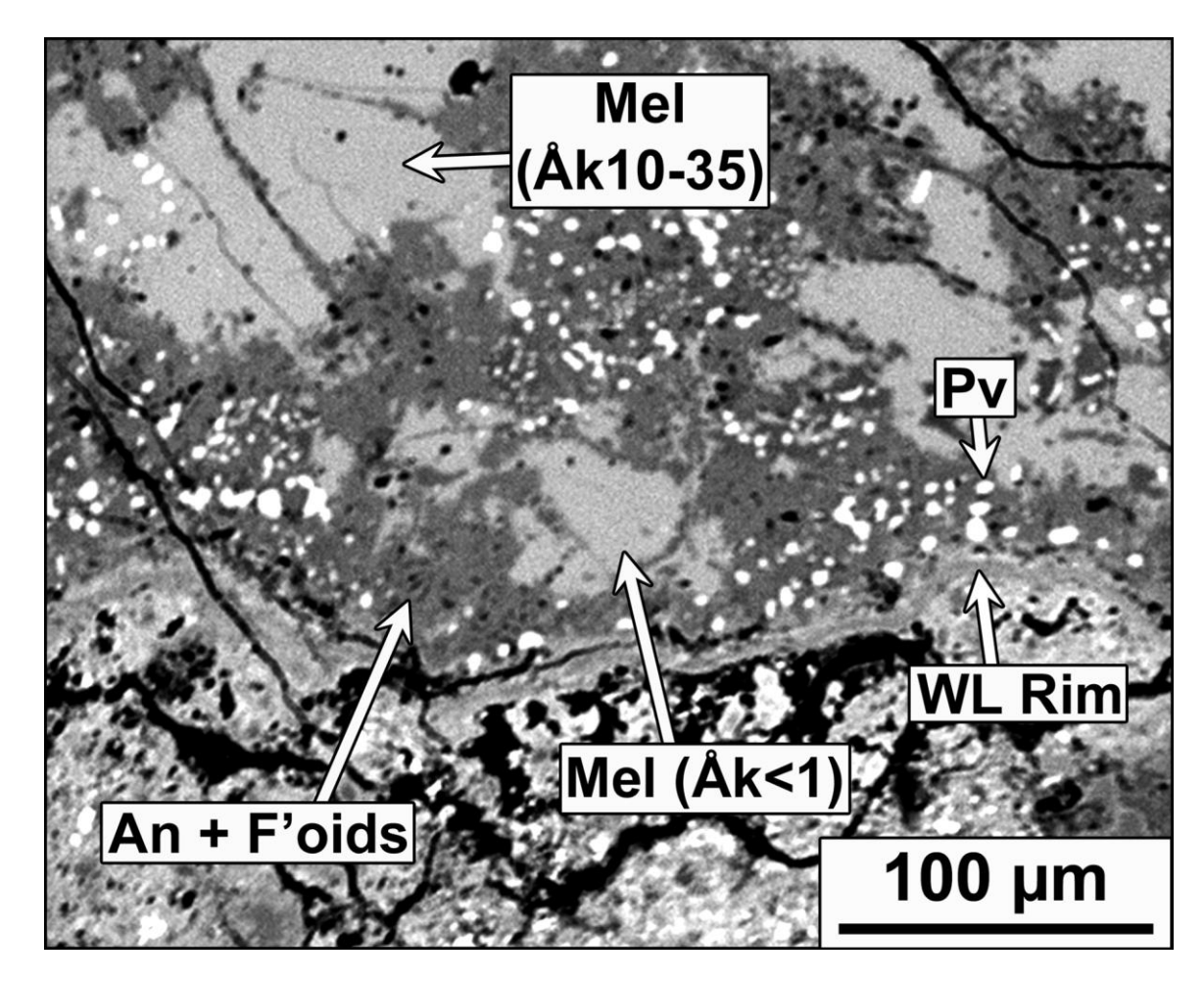


Figure 3. Detailed BSE image of the outermost edge of USNM 3898, showing the presence of very aluminous melilite just inside the Wark-Lovering rim sequence (WL-Rim). Melilite more distant from the edge is more magnesium-rich. Abbreviations as used previously except: Åk – Åkermanite, which expresses the melilite composition in terms of mole percent of the magnesium end member åkermanite.

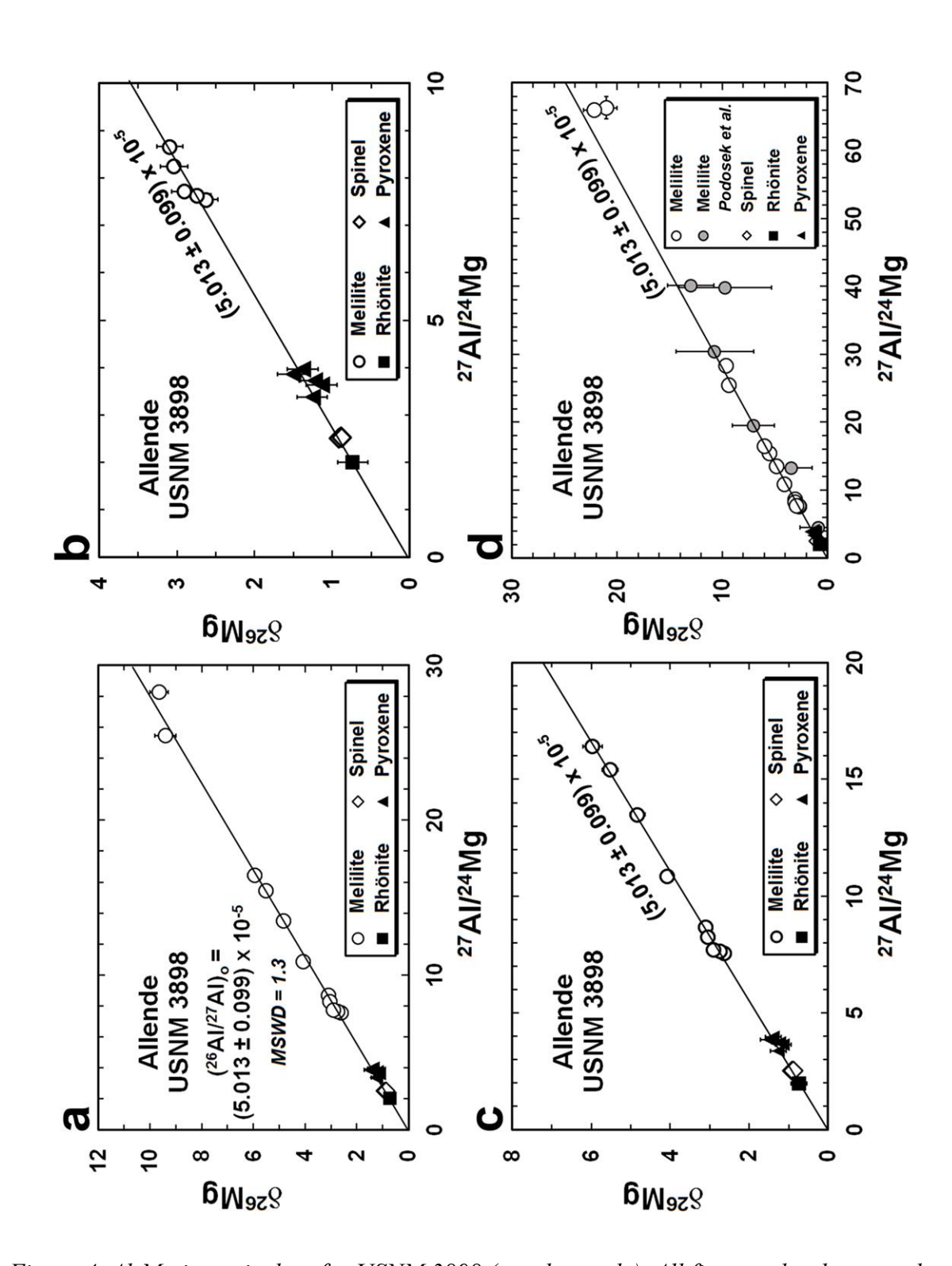


Figure 4. Al-Mg isotopic data for USNM 3898 (our data only). All figures plot the same data but at different scales. Error bars (2 $\sigma$ ) are mostly smaller than data symbols. The isochrons shown in Figs. 4b-4c are the same as that shown in Fig. 4a.

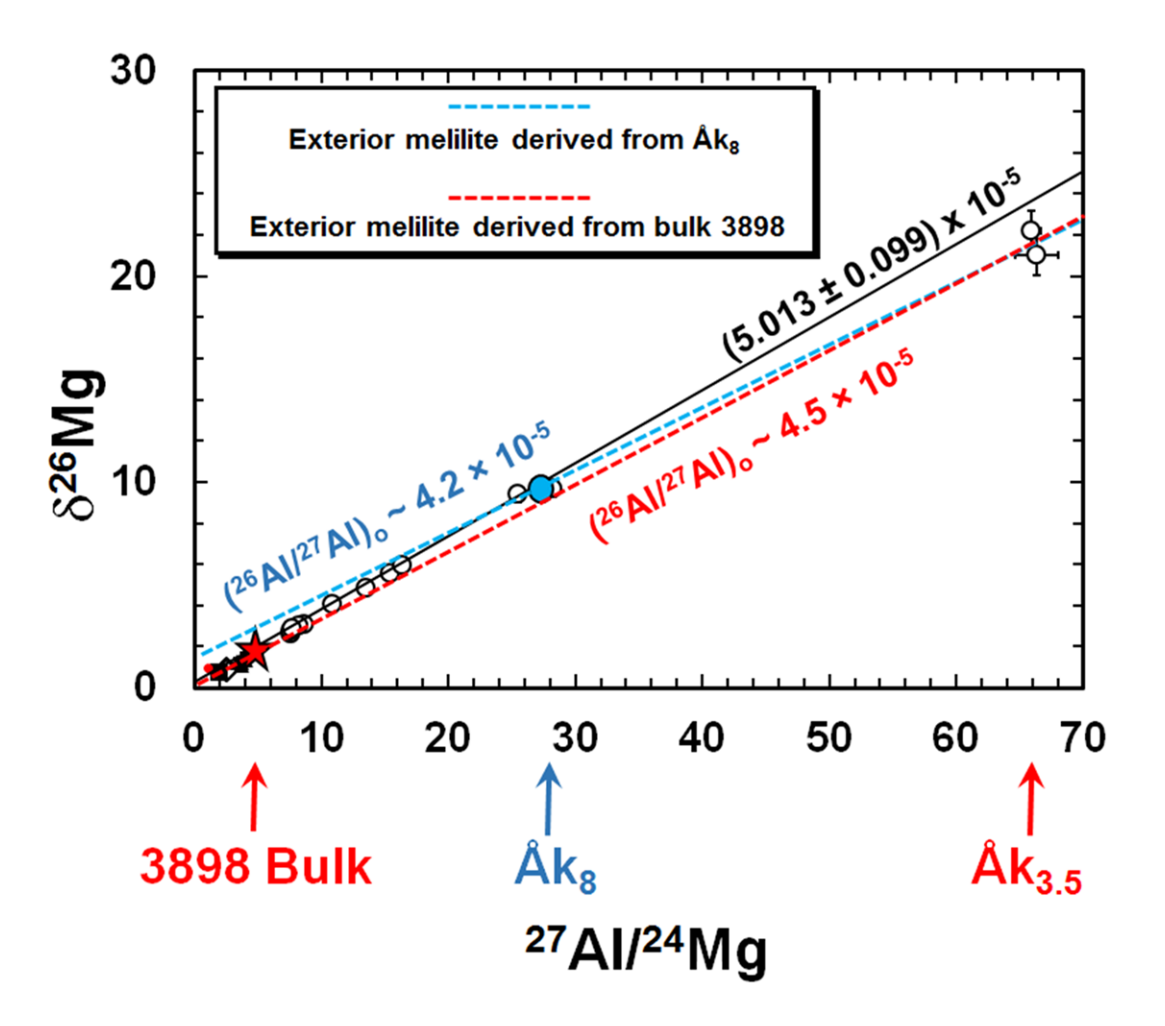


Figure 5. Two possible cases for the isotopic evolution of melilite in the outermost mantle of USNM 3898 following melt evaporation, assuming the composition of the evaporating melt had the  $^{27}Al/^{24}Mg$  of either (a) the bulk CAI (in red) or (b) the composition of the most aluminous melilite that is isotopically concordant with all interior phases, Åk<sub>8</sub> (in blue).

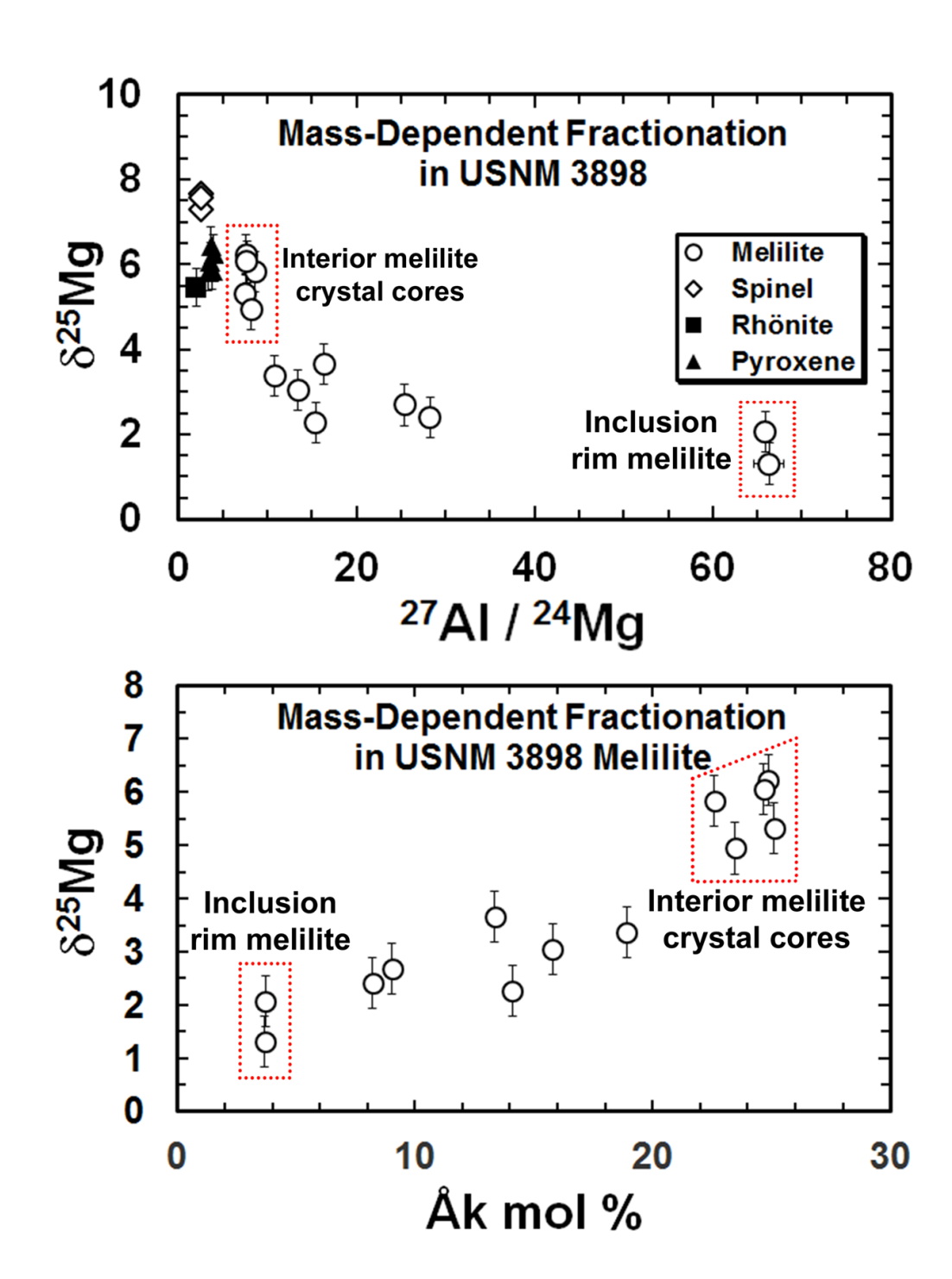


Figure 6. Intrinsic mass-dependent fractionation in USNM 3898 (a) in all phases as a function of  $^{27}Al/^{24}Mg$ , and (b) in melilite only, as a function of melilite composition expressed in terms of mole percent åkermanite (Åk). The highest degree of heavy isotope enrichment is in interior pyroxene, spinel, rhönite, and in the cores of reversely-zoned melilite crystals. The lowest degree of fractionation is in the very aluminous melilite located near the inclusion rim.